



Chronic Benzene Exposure Aggravates Pressure Overload-Induced Cardiac Dysfunction

Igor N. Zelko ,^{*,†,‡,§,1} Sujith Dassanayaka,^{†,§} Marina V. Malovichko,^{*,†,‡,§} Caitlin M. Howard,^{†,‡,§} Lauren F. Garrett,^{†,‡,§} Shizuka Uchida ,[¶] Kenneth R. Brittan,^{†,‡,§} Daniel J. Conklin,^{*,†,‡,§} Steven P. Jones,^{†,‡,§} and Sanjay Srivastava^{*,†,‡,§,1}

^{*}Superfund Research Center, University of Louisville, Louisville, Kentucky 40202, USA; [†]Diabetes and Obesity Center, University of Louisville, Louisville, Kentucky 40202, USA; [‡]Envirome Institute, University of Louisville, Louisville, Kentucky 40202, USA; [§]Division of Environmental Medicine, Department of Medicine, University of Louisville, Louisville, Kentucky 40202, USA; and [¶]Department of Clinical Medicine, Center for RNA Medicine, Aalborg University, Copenhagen, SV, Denmark

Dryad Digital Repository DOI: 5061/dryad.12jm63xz6

¹To whom correspondence should be addressed at Division of Environmental Medicine, Department of Medicine, University of Louisville Room 310 CII Building, 302 E. Muhammad Ali Blvd, Louisville, KY 40202, USA. E-mail: igor.zelko@louisville.edu and Superfund Research Center, University of Louisville, Room 306 CII Building, 302 E. Muhammad Ali Blvd, Louisville, KY 40202, USA. Fax: (502) 852-5834. E-mail: sanjay@louisville.edu.

ABSTRACT

Benzene is a ubiquitous environmental pollutant abundant in household products, petrochemicals, and cigarette smoke. Benzene is a well-known carcinogen in humans and experimental animals; however, little is known about the cardiovascular toxicity of benzene. Recent population-based studies indicate that benzene exposure is associated with an increased risk for heart failure. Nonetheless, it is unclear whether benzene exposure is sufficient to induce and/or exacerbate heart failure. We examined the effects of benzene (50 ppm, 6 h/day, 5 days/week, and 6 weeks) or high-efficiency particulate absorbing-filtered air exposure on transverse aortic constriction (TAC)-induced pressure overload in male C57BL/6J mice. Our data show that benzene exposure had no effect on cardiac function in the Sham group; however, it significantly compromised cardiac function as depicted by a significant decrease in fractional shortening and ejection fraction, as compared with TAC/Air-exposed mice. RNA-seq analysis of the cardiac tissue from the TAC/benzene-exposed mice showed a significant increase in several genes associated with adhesion molecules, cell-cell adhesion, inflammation, and stress response. In particular, neutrophils were implicated in our unbiased analyses. Indeed, immunofluorescence studies showed that TAC/benzene exposure promotes infiltration of CD11b⁺/S100A8⁺/myeloperoxidase⁺-positive neutrophils in the hearts by 3-fold. *In vitro*, the benzene metabolites, hydroquinone, and catechol, induced the expression of P-selectin in cardiac microvascular endothelial cells by 5-fold and increased the adhesion of neutrophils to these endothelial cells by 1.5- to 2.0-fold. Benzene metabolite-induced adhesion of neutrophils to the endothelial cells was attenuated by anti-P-selectin antibody. Together, these data suggest that benzene exacerbates heart failure by promoting endothelial activation and neutrophil recruitment.

Key words: benzene; heart failure; adhesion molecules; endothelial cells; neutrophils; RNA-seq.

Environmental pollution is a health problem worldwide. More than 9 million premature deaths are attributed to pollution every year, out of which 6 million deaths are related to air pollution (Collaborators, 2016). Nearly, half of the air pollution-associated deaths are ascribed to cardiovascular disease (Collaborators, 2016). Cardiovascular health effects of criteria pollutants (particulate matter_{2.5}, sulfur dioxide, carbon monoxide, nitrogen oxides, ozone, and lead) have been extensively studied in the last 3 decades; however, information about the potential cardiovascular toxicity of other airborne chemicals, such as volatile organic compounds (eg, benzene, 1,3-butadiene, vinyl chloride, trichloroethylene, etc.), is sparse. Benzene, a well-known carcinogen, is abundant in household products, cigarette smoke, and automobile exhaust (Appel et al., 1990; Clayton et al., 1999; Fraser et al., 1998; Jacob et al., 2013), and the atmospheric concentration of benzene can exceed 50 ppm, especially near the emission source. People working at gasoline pumping stations or living near hazardous waste sites can be exposed to high levels of benzene. The U.S. Occupational Safety and Health Administration has set the occupational benzene exposure limit of 1 ppm (Smith, 2010); however, occupational benzene exposure in excess of 100 ppm has been reported in developing countries (Wong and Fu, 2005).

Like pollution, heart failure is a pervasive health problem. Heart failure affects more than 6.5 million people in the United States (Benjamin et al., 2017) and 26 million people worldwide (Ponikowski et al., 2014). The lifetime risk for heart failure at 40 years of age is estimated to be 1 in 5 people (Lloyd-Jones et al., 2002). The pathogenesis of heart failure is also not clearly understood, although a substantial body of literature points to the important role of infiltrating immune cells in the development of left ventricular hypertrophy and cardiac dysfunction (Bajpai et al., 2018; Kain et al., 2016; Liao et al., 2018; Marinkovic et al., 2019; Nahrendorf et al., 2007; Patel et al., 2017; Sager et al., 2016; Weisheit et al., 2014). Therefore, the current focus in finding new therapeutic approaches to delay advanced heart failure includes understanding the molecular mechanisms that govern cardiomyocyte interactions with immune cells (Halade et al., 2018; Martini et al., 2019; Weinberger and Schulz, 2015). The innate immune response induced by heart failure initiates the cardiac repair process, and involves infiltration of peripheral neutrophils (Horckmans et al., 2017; Lindsey et al., 2016; Ma et al., 2016).

Recent population-based studies have reported that benzene exposure is associated with an increased risk for heart failure (Ran et al., 2018), and presence of mono-nitrogen oxide and benzene in the air of hospital wards is associated with a higher risk of heart failure morbidity (Bennett et al., 2014). Other studies have linked exposure to benzene with cardiovascular mortality (Tsai et al., 2010; Villeneuve et al., 2013); however, direct effects of benzene exposure on heart failure in well-controlled animal studies have not been studied. Here, we examined the effect of chronic benzene exposure on transverse aortic constriction (TAC)-induced cardiac function and associated immune response in mice.

MATERIALS AND METHODS

Reagents. Benzene permeation tubes were obtained from Kin-Tek (La Marque, Texas). Primers and probes for real-time PCR were purchased from Integrated DNA Technologies (Coralville, Iowa) and ThermoFisher Scientific (Waltham, Massachusetts). Sources of antibodies used for immunohistochemistry and functional studies were: anti-CD11b (Abcam, cat No. ab1333357,

RRID: AB_2650514), anti-myeloperoxidase (Abcam, cat No. ab9535, RRID: AB_307322); anti-S100A8 (63N13G5)-FITC (Novus, cat No. NBP2-25273F); anti-CD90/Thy1 (Sino Biological, cat No. 50461-T44); CD62P (Biolegend, cat No. 148308, RRID: AB_2565817). Murine cardiac microvascular endothelial cells (CMVECs) were obtained from CellBiologics, Chicago, IL. All other chemicals and enzymes were from Sigma Chemical Co. (St Louis, Missouri), or Invitrogen (Carlsbad, California).

Animal housing and maintenance. C57BL/6J male mice obtained from Jackson Laboratory (Bar Harbor, Maine) were maintained on normal chow in a pathogen-free facility accredited by the Association for Assessment and Accreditation of Laboratory Animal Care. All procedures were approved by the University of Louisville Institutional Animal Care and Use Committee. We used male mice in our study because multiple studies have shown that rate of benzene metabolism, and consequently benzene toxicity, is significantly higher in male mice than in female mice (Bauer et al., 2003; Kenyon et al., 1998; Ward et al., 1985).

Animal surgeries. For TAC (Baba et al., 2018), male C57BL/6J mice 12 weeks of age were anesthetized (intraperitoneal injections of 50 mg/kg sodium pentobarbital and 50 mg/kg ketamine hydrochloride), antiseptically prepared for surgery, orally intubated, and ventilated (oxygen supplement to the room-air inlet) with a mouse ventilator (Hugo Sachs). Core body temperature was maintained at 36.5°C–37.5°C with an automatic, electronically regulated heat lamp. The aorta was visualized following an intercostal incision. A 7-0 nylon suture was looped around the aorta between the brachiocephalic and left common carotid arteries. The suture was tied around a 27-gauge needle placed adjacent to the aorta to constrict the aorta to a reproducible diameter. The needle was removed, and the chest was closed in layers. Mice were extubated upon recovery of spontaneous breathing. Analgesia (ketoprofen, 5 mg/kg) was provided prior to recovery and by 24 and 48 h postsurgery. Sham mice were subjected to the same procedure as the TAC cohort except the suture was not tied.

Benzene exposure. One week after the TAC, mice were exposed to benzene for 6 weeks in bedding-free cages as described before (Lang et al., 2018). Briefly, benzene atmospheres were generated from liquid benzene (Sigma-Aldrich) in a KIN-TEK Analytical, Inc permeation tube. A carrier gas (N₂) was delivered to the permeation tube at 100 ml/min and diluted with HEPA (high-efficiency particulate absorbing)- and charcoal-filtered room air (3 l/min) and diluted gas directed to an exposure unit. Flow was distributed through a fine mesh screen of a custom cyclone-type top (Teague Enterprises) that distributed air within 10% of the mean concentration at 6 locations in the cage. Throughout the exposure, benzene concentrations were continuously monitored using an in-line photoionization detector (ppb RAE: Rae Industries) upstream of the exposure unit. Mice were exposed to 50 ppm benzene (6 h/day, 5 days/week) for 6 weeks. Mice exposed to HEPA- and charcoal-filtered room air only were used as controls.

Echocardiography. At the end of the benzene exposure protocol, mice were anesthetized with 2% isoflurane, and echocardiography was performed (VisualSonics Vevo 3100), similar to our previous reports (Baba et al., 2018; Dassanayaka et al., 2018). At the end of the experiment, hearts were excised for biochemical and pathological analyses. For mice in the TAC arm of the study,

Doppler verification of the stenosis was used. The sonographer was blinded to the specific experimental group.

RNA isolation and RNA-seq analysis. Total RNA was extracted from the hearts of mice using TRIzol kit (ThermoFisher Scientific), and the purity of RNA was analyzed using NanoDrop One (ThermoFisher Scientific). RNA quality was measured by Agilent 2100 bioanalyzer (Thermo Fisher Scientific) and samples with high RNA integrity were used for subsequent RNA-seq analysis. RNA samples were processed by Novogene using mRNA and small RNA sequencing services (Novogene, Beijing, China). The resultant raw reads of the FASTQ files were processed and quality metrics were visualized using FastQC v 0.11.9. The mRNA differentially regulated genes (DEGs) and pathway enrichment analysis were performed using the NGS Data Analysis pipeline (An et al., 2020). RNA-seq data have been submitted to the DRYAD database: <https://datadryad.org/stash/share/aTPKrma2a7Sppu2N3HoVdezhPpVdUncU8PI1cuxz1q8>.

Histopathology. Formalin-fixed, paraffin-embedded hearts from Sham and TAC mice were sectioned at 4- μ m thickness, and later deparaffinized, and rehydrated according to the appropriate staining method. The histological staining was performed as previously described (Watson et al., 2010, 2014). Picro-Sirius Red staining was used to evaluate tissue fibrosis and general histology, and Alexa Fluor 555-conjugated wheat-germ agglutinin (Invitrogen) staining was used to determine the average myocyte area. All images were captured at 20 \times magnification using the Keyence BZ-X810, all in 1 fluorescent microscope. Both fibrosis and myocyte areas were analyzed using the hybrid cell count feature (BZ-H4C) associated with the Keyence system. Fibrosis was expressed as a percentage of scar tissue divided by the total area of tissue.

Immunofluorescence. For immunostaining, deparaffinized and rehydrated sections were incubated for 20 min with 10 mmol/l citric acid pH 6.0 (pH 9.0 for MPO staining). Nonspecific binding was blocked with 5% normal goat serum and 0.05% saponin (Sigma) in PBS (pH 7.4) for 30 min. Sections were blocked and then incubated with the appropriate primary antibody in PBS with 1% BSA and 0.05% saponin for 1 h at 37°C against: CD11b (1:100 dilution), S100A8-FITC (1:200 dilution), myeloperoxidase (1:25 dilution), CD90/Thy1 (1:200 dilution). Tissue sections were then incubated for 30 min at room temperature with respective secondary antibodies conjugated with Alexa 488, 555, or 647 (Invitrogen), and counterstained with DAPI to label nuclei. Heart sections stained with nonimmune primary antibody or only fluorophore-labeled secondary antibodies served as negative controls. Images were made with a 20 \times and 60 \times objective.

Neutrophils isolation. Neutrophils were isolated from bone marrow as described previously (Swamydas et al., 2015). Briefly, C57BL6/J male mice 10 weeks old were sacrificed using pentobarbital injection. Bone marrow cells were flushed from the femur and tibia and filtered through a 70- μ m mesh filter. For a negative selection of neutrophils, we used a Neutrophil Isolation kit from Miltenyi, Auburn, California. Magnetic sorting was performed using MS columns. Neutrophils presented in flow-through fractions were characterized using flow cytometry and by cytochrome with Diff-Quick staining. Neutrophil purity was always higher than 93%.

Cell adhesion assay. Neutrophil adhesion to CMVEC was determined as previously described (Wilhelmsen et al., 2013). Briefly,

CMVEC (passages 6–10) were seeded into 96-well plates at 25 000 cells per well in 100 μ l of growth media. Twenty-four hours later confluent monolayer of endothelial cells was exposed to benzene metabolite catechol (5 μ M) for 24 h. Cells treated with tumor necrosis factor alpha TNF- α (100 ng/ml) for 4 h served as positive controls. Isolated neutrophils labeled with calcein (Wilhelmsen et al., 2013) were added to endothelial cells and incubated for 30 min at 37°C. Cells were rinsed with PBS containing Mg²⁺ and Ca²⁺ and the fluorescence was measured with a Synergy H1 (Biotek) fluorescence plate reader (excitation wavelength, 485 nm and emission wavelength, 520 nm). To measure the effect of p-selectin blocking on neutrophil adhesion, CMVEC were incubated with anti-CD62P antibodies (25 μ g/ml) for 30 min prior to the neutrophil adhesion assay. For each assay, 10–12 wells were used.

Statistical analyses. Data are presented as means \pm SEM. Statistical analyses for echo-based parameters were performed after adjustment for body weight and heart rate by 2-way analysis of variance (ANOVA) with Tukey-Kramer corrections. A 2-way ANOVA with Tukey post hoc test was also used for the analyses of RNA-seq, histopathology, and immunofluorescence data. *In vitro* data were analyzed by 1-way ANOVA with Holm-Sidak post hoc test to compare differences between multiple experimental groups. A *p*-value of < .05 indicated statistically significant differences. All analyses were performed using Excel and GraphPad Prism software (GraphPad Software, San Diego, California).

RESULTS

Benzene Exposure Exacerbates Pressure Overload-Induced Cardiac Dysfunction

As expected, mice in the TAC/Air group developed significant left ventricular dilation as indicated by a significant increase in end-diastolic volume (EDV), end-systolic volume (ESV), left ventricular internal diameter in diastole (LVIDd), diameter in systole (LVIDs), consequent decrease in fractional shortening (FS), and ejection fraction (EF), as compared with the mice in corresponding Sham/Air (Figure 1). TAC also increased the heart mass, cardiac myocyte size and fibrosis in the heart (Figure 1). This was accompanied with a significant increase in the fluid accumulation in the lung (Supplementary Figure 1). Benzene exposure had no effect on myocyte size and cardiac function in the Sham group; however, it significantly compromised cardiac function as depicted by a significant increase in EDV, ESV, LVIDd, and LVIDs and resultant decrease in FS and EF, as compared with TAC/Air-exposed mice (Figure 1 and Supplementary Table 1). The other cardiac function parameters such as left ventricular anterior wall thickness at diastole or systole and left ventricular posterior wall thickness at diastole or systole, isovolumic relaxation time, stroke volume, and cardiac output did not significantly change in TAC/Benzene versus TAC/Air groups (Supplementary Table 1). Cardiac myocyte size and fibrosis in TAC/Benzene-exposed mice were also comparable with the TAC/Air-exposed mice. Collectively, these data suggest that a 6-week benzene exposure exacerbates TAC-induced cardiac dysfunction but does not induce cardiac remodeling in Sham mice.

RNA-Seq Analyses of TAC-Benzene-Exposed Hearts

To examine the molecular mechanisms by which benzene worsens cardiac function following TAC, we performed deep RNA sequencing on the left ventricle and septum tissues. For these

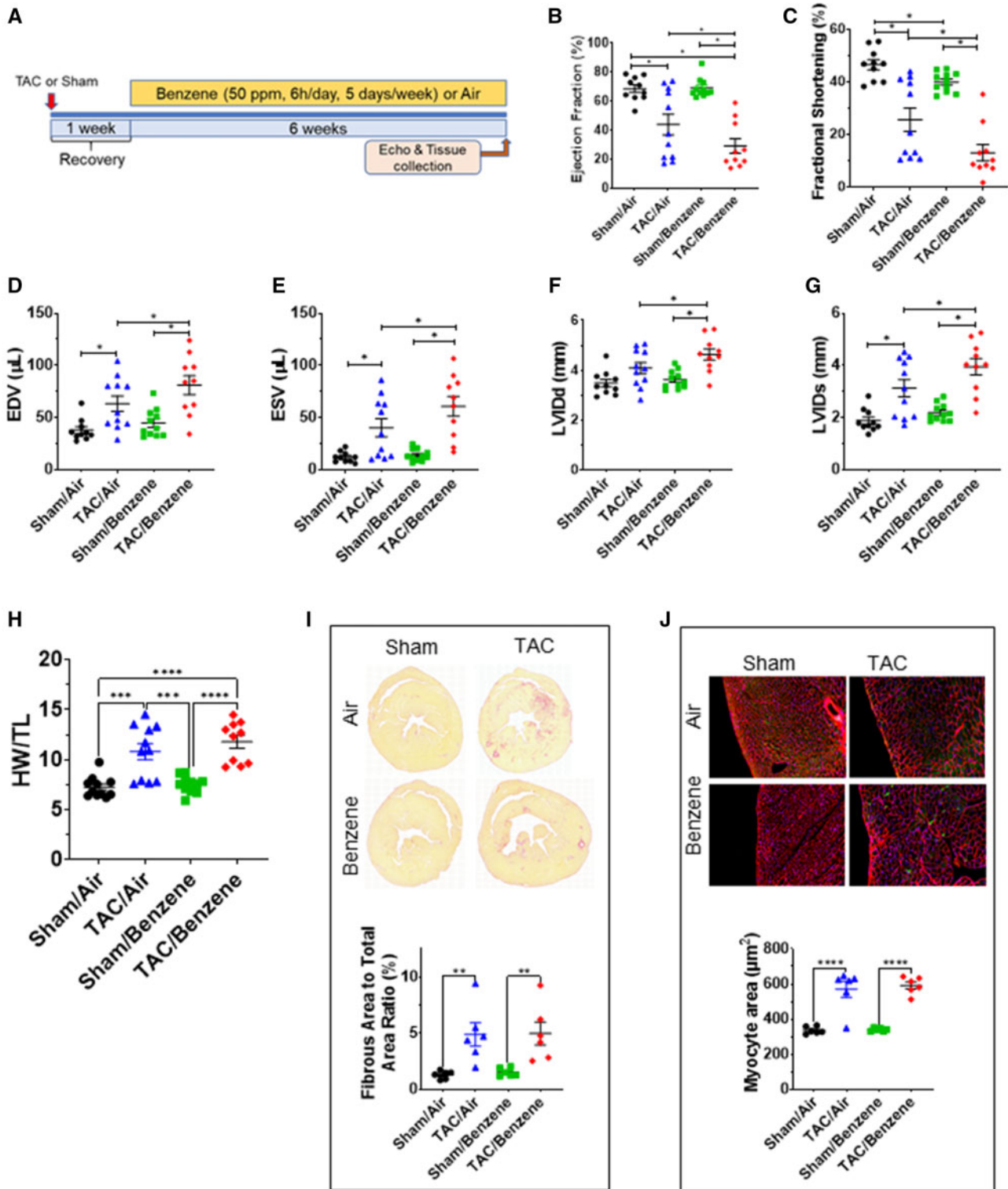


Figure 1. Effect of benzene exposure on left ventricle function and cardiac remodeling after pressure overload. **A**, Benzene exposure protocol: Transverse aortic constriction or Sham-operated male C57BL/6 mice were exposed to benzene (50 ppm, 6 h/day, 5 days/week) or HEPA-filtered air (Air) for 6 weeks. At the end of the exposure protocol, echocardiography was used to measure ejection fraction (**B**), fractional shortening (**C**), end-diastolic volume (EDV; **D**), end-systolic volume (ESV; **E**), left ventricular internal diameter end diastole (LVIDd; **F**) and end systole (LVIDs; **G**). Heart weight: tibial length (TL) are presented in (**H**). Statistical analyses for echo-based parameters were performed after adjustment for body weight and heart rate by 2-way ANOVA with Tukey-Kramer corrections. **I**, The representative images of Sirius Red-stained mid-ventricular histological sections from mouse hearts with quantitative analysis of fibrosis expressed as percent of fibrous area to total area ratio. Representative images of wheat germ agglutinin-stained mid-ventricular histological sections from mouse hearts with quantitative analysis of myocyte area are illustrated in panel **J**. Values are mean \pm SEM. * $p < .05$, ** $p < .01$, *** $p < .001$, **** $p < .0001$ represent statistical significance between corresponding groups analyzed by 2-way ANOVA with Tukey post hoc test ($n = 6-11/\text{group}$).

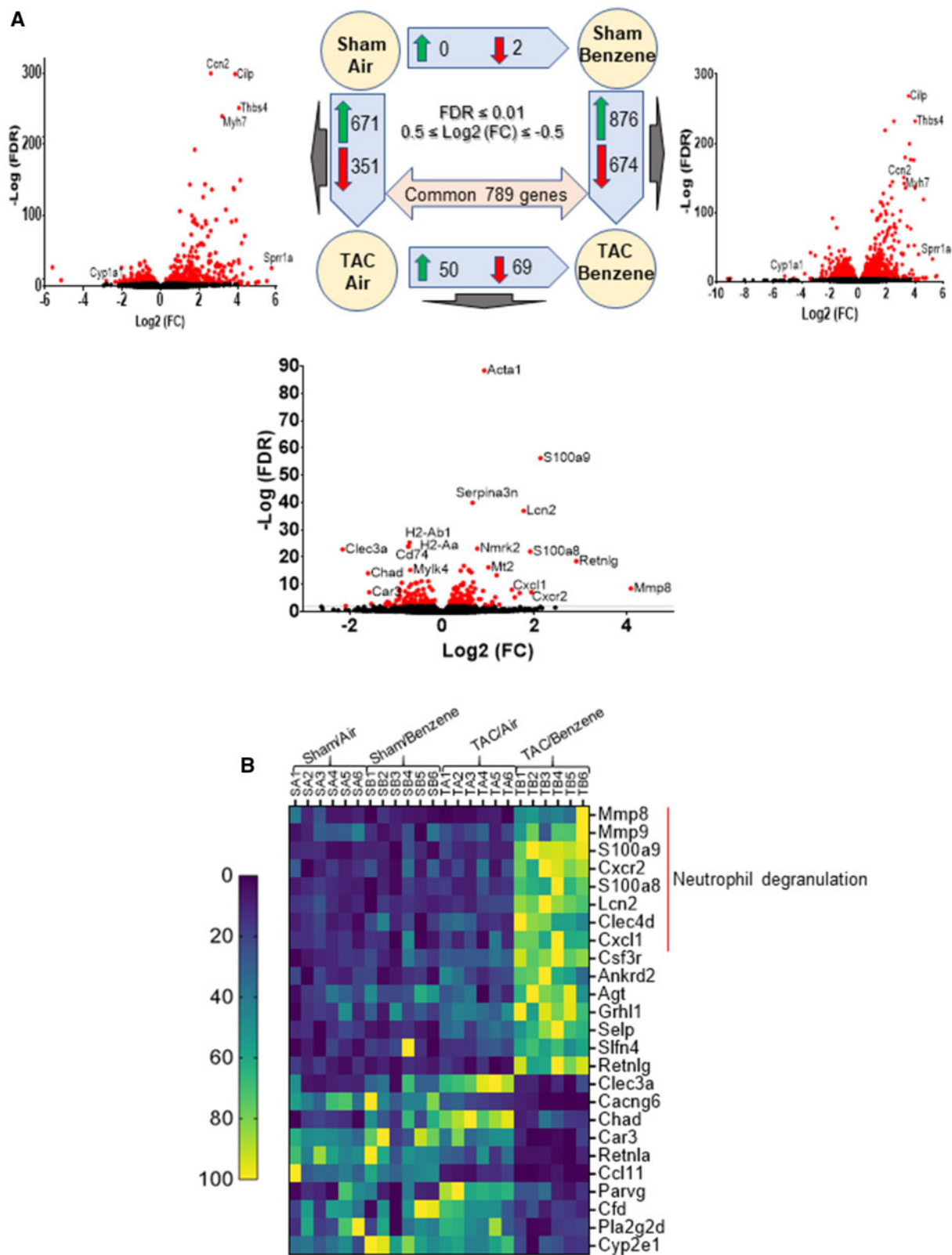


Figure 2. Differential expression of genes (DEGs) in the hearts of transverse aortic constriction (TAC)/Benzene-exposed mice. **A**, The number of DEGs are depicted by corresponding arrows. The visual representation of DEG for 3 treatments is presented as volcano plots ($FDR \leq 0.01$). **B**, Heatmap of the top 15 upregulated and 10 down-regulated (TAC/Benzene vs. TAC/Air) protein-encoding genes in the 4 experimental groups.

analyses, we used false discovery rate (FDR) ≤ 0.01 and $0.5 \leq \text{Log}_2(\text{fold change}) \leq -0.5$ to examine the differential expression of the genes. As shown in Figure 2A, TAC upregulated 671 genes (eg, genes involved in extracellular matrix organization and collagen formation) and downregulated 351 genes (eg, genes involved in muscle contraction and cardiac conduction) in the air-exposed mice (see Supplementary Table 2). Exposure to benzene in Sham-operated mice did not induce any genes while uteroglobin (*Scgb1a1*) and surfactant protein C (*Sftpc*) were downregulated by 8.9- and 6.1-fold. However, benzene exposure in TAC mice significantly upregulated 876 genes and downregulated 674 genes as compared with the corresponding Sham-operated controls. Comparison of the gene expression between TAC/Benzene versus TAC/Air mice showed upregulation of 50 and downregulation of 69 genes. Figure 2B illustrates the heatmap of top the 15 upregulated and 10 downregulated genes between these groups as well as the differential expression of these genes in the other experimental groups. Gene ontology of biological process and molecular function enrichment analyses of differentially expressed genes in the benzene-exposed TAC hearts show significant enrichment of the genes associated with the regulation of “neutrophil degranulation,” “signaling by interleukins,” “extracellular matrix organization,” “platelet degranulation,” and heat shock factor-1 (HSF-1)-dependent transactivation, etc. (Figure 3A). Figure 3B shows the induction of some representative genes of these processes, and Figure 3C displays the gene-concept network of select differentially expressed genes associated with the indicated biological pathways including neutrophil degranulation, interleukin (IL) signaling, and HSF-1 activation.

Benzene Exposure Augments TAC-Induced Neutrophil Infiltration

Because our RNA-Seq data suggest that benzene exposure affects inflammatory response and neutrophil degranulation processes in TAC hearts, we examined the abundance of inflammatory cells in the TAC/benzene-exposed hearts. As shown in Figure 4a, benzene exposure induced massive infiltration of S100A8-positive granulocytes in the hearts of TAC mice. These cells also co-stained with the pan-myeloid marker CD11b and myeloperoxidase, mostly expressed on neutrophils (Figs. 4A and 4B). Quantitative analysis shows >3-fold increase in S100A8⁺ granulocytes, CD11b⁺ myeloid cells, and myeloperoxidase⁺ neutrophils in TAC/Benzene versus TAC/Air groups (Figure 4C). The S100A8 staining did not co-localize with the markers of CD68⁺ macrophages and Thy1⁺ fibroblasts in TAC-Benzene hearts (Supplementary Figure 2). To examine the mechanisms by which benzene exposure augments neutrophil infiltration in TAC-instrumented hearts, we analyzed the RNA-seq data for the differential expression of adhesion molecules. As shown in Figure 4D, benzene exposure did not affect the levels of adhesion molecules in the Sham-operated hearts; however, it significantly increased the transcription of Intracellular adhesion molecule-1 (*Icam1*), endothelial-selectin (*Sele*), and platelet-selectin (*Selp*) genes in the TAC-instrumented hearts. Expression of vascular cell adhesion molecule (*Vcam1*) in TAC-benzene hearts was comparable with the TAC/Air hearts. Together, these data indicate that chronic benzene exposure enhances the infiltration of neutrophils, possibly by activating adhesion molecules in the myocardial endothelial cells during pressure overload-induced cardiac dysfunction.

P-Selectin Facilitates the Adhesion of Neutrophils Adhesion to the CMVECs

Complimentary *in vitro* experiments with CMVEC showed that benzene metabolites hydroquinone (5 μM , 24 h) and catechol (5 μM , 24 h) increased the transcription of P-selectin by 5-fold (Figure 5A) and abundance of P-selectin protein by 1.5-2-fold (Figure 5B). Incubation of CMVEC with catechol for 24 h augmented the adhesion of bone marrow-derived neutrophils to CMVEC (Figure 5C), which was attenuated by pre-incubation of CMVEC with anti-P-selectin antibody (Figure 5D). Hydroquinone and catechol also increased the expression of IL8 (Supplementary Figure 3), which can function both as a membrane-bound and soluble activator of neutrophil β_2 integrin-mediated adhesion. Together, these observations suggest that benzene-induced neutrophil infiltration in the TAC hearts could be facilitated, at least in part, by the metabolic conversion of benzene to its active metabolites- hydroquinone and catechol.

DISCUSSION

The major finding of this study is that chronic benzene exposure exacerbates pressure overload-induced cardiac dysfunction. The TAC/Benzene-induced cardiac dysfunction is accompanied by endothelial activation and enhanced recruitment of granulocytes in the heart and differential regulation of genes involved in neutrophil degranulation, inflammatory signaling, and stress response. These studies corroborate recent reports that occupational and environmental exposure to benzene is associated with an increased risk for heart failure (Ran et al., 2018).

Inflammatory processes have long been implicated in the manifestation, progression, and consequences of ischemic heart disease (Silvestre-Roig et al., 2020; Swirski and Nahrendorf, 2018) and pressure- or volume overload-induced mechanical stress (Frangogiannis, 2017; Hutchinson et al., 2010; Wang et al., 2019; Weisheit et al., 2014). Pressure overload induces the expression of ICAM1 (Salvador et al., 2016) and consequent increase in the recruitment of neutrophils in the heart (Wang et al., 2019) and subsequent monocyte infiltration (Wang et al., 2019; Weisheit et al., 2014;). It diminishes TAC-induced cardiac hypertrophy and inflammation and sustains cardiac function (Wang et al., 2019), suggesting that neutrophils play a pivotal role in the manifestation of heart disease, especially heart failure. In mice, increased recruitment of S100A9 positive granulocytes, which costained with myeloperoxidase, suggests that TAC/Benzene exposure facilitates the infiltration of neutrophils into the hearts.

This is further supported by RNA-seq data of cardiac tissue, demonstrating robust induction in the neutrophil-specific S100A8/A9, *Mmp8*, *Lcn2*, and *Cxcr2* transcripts. S100A8/A9 is a member of alarmins or damage-associated molecular patterns (DAMPs) that are released by the failing heart (Bliksoen et al., 2016; Krysko et al., 2011; Lipps et al., 2016) and subsequently activate resident macrophages, fibroblasts, and endothelial cells to secrete proinflammatory cytokines and adhesion molecules (Shioi et al., 1997) and augment inflammation in the cardiac tissue (Horckmans et al., 2017; Martini et al., 2019; Patel et al., 2018). Systemic administration of S100A8/A9 facilitates the mobilization of neutrophils from the bone marrow (Vandal et al., 2003), whereas local administration of S100A8/A9 leads to rapid recruitment of monocytes and neutrophils into the site of injury (Ryckman et al., 2003). Patients with myocardial infarction and elevated S100A8/A9 levels have poorer prognosis (Healy et al.,

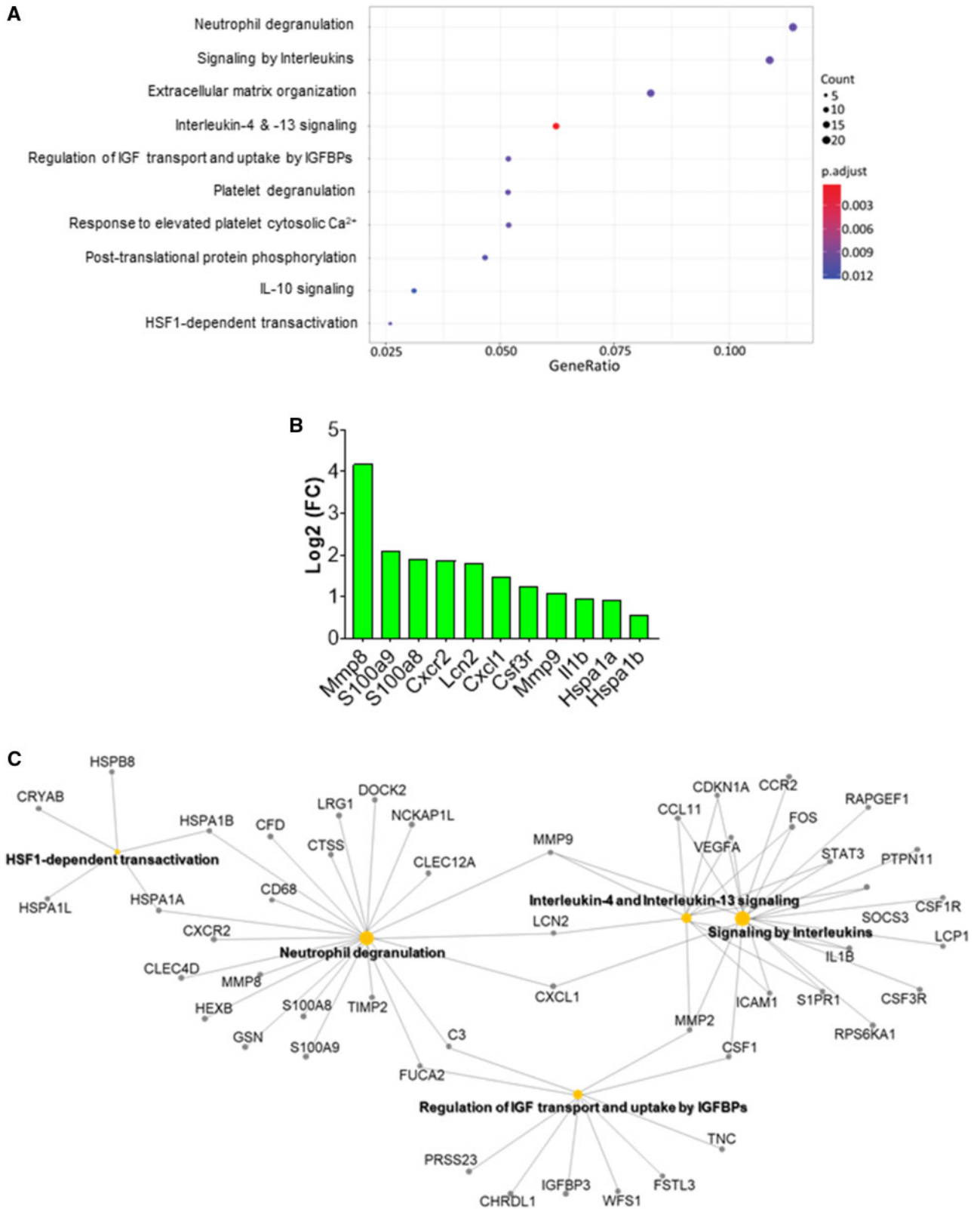


Figure 3. Pathway enrichment analysis of differentially expressed genes (DEGs) in the hearts of transverse aortic constriction (TAC)/Benzene-exposed mice. A, Dot plot of enriched terms for TAC/Benzene versus TAC/Air DEG (FDR ≤ 0.01). Abbreviations: IGF, insulin-like growth factor; IGFbps, insulin-like growth factor binding proteins. B, The most upregulated and functionally important genes in TAC/Benzene versus TAC/Air groups. C, Gene-concept network depicting the linkage of genes and enriched biological pathways as a network.

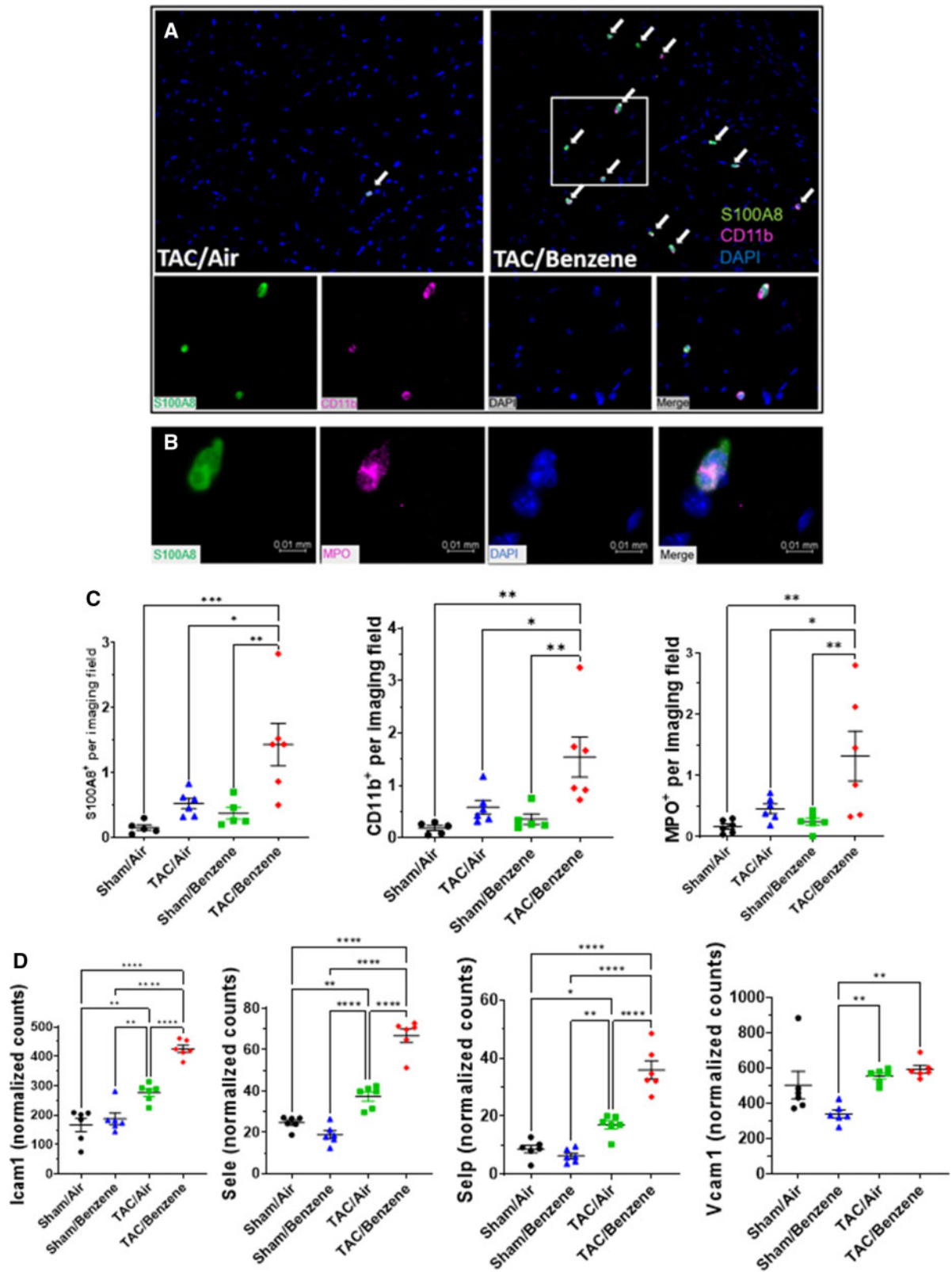


Figure 4. Immune cells infiltration into the heart of transverse aortic constriction (TAC)/Benzene-exposed mice. **A**, Heart sections were stained for S100A8 (green) and CD11b (pink), nuclei (blue). **B**, Costaining of S100A8 positive cells with myeloperoxidase (MPO) positive cells. **C**, Quantitative analysis of S100A8-, CD11b-, and MPO-positive cells. **D**, Expression levels of adhesion genes in the hearts of exposed mice. Values are mean \pm SEM. * $p < .05$, ** $p < .01$, and *** $p < .001$ represent statistical significance between corresponding groups analyzed by 2-way ANOVA with Tukey post hoc test ($n = 6$ /group).

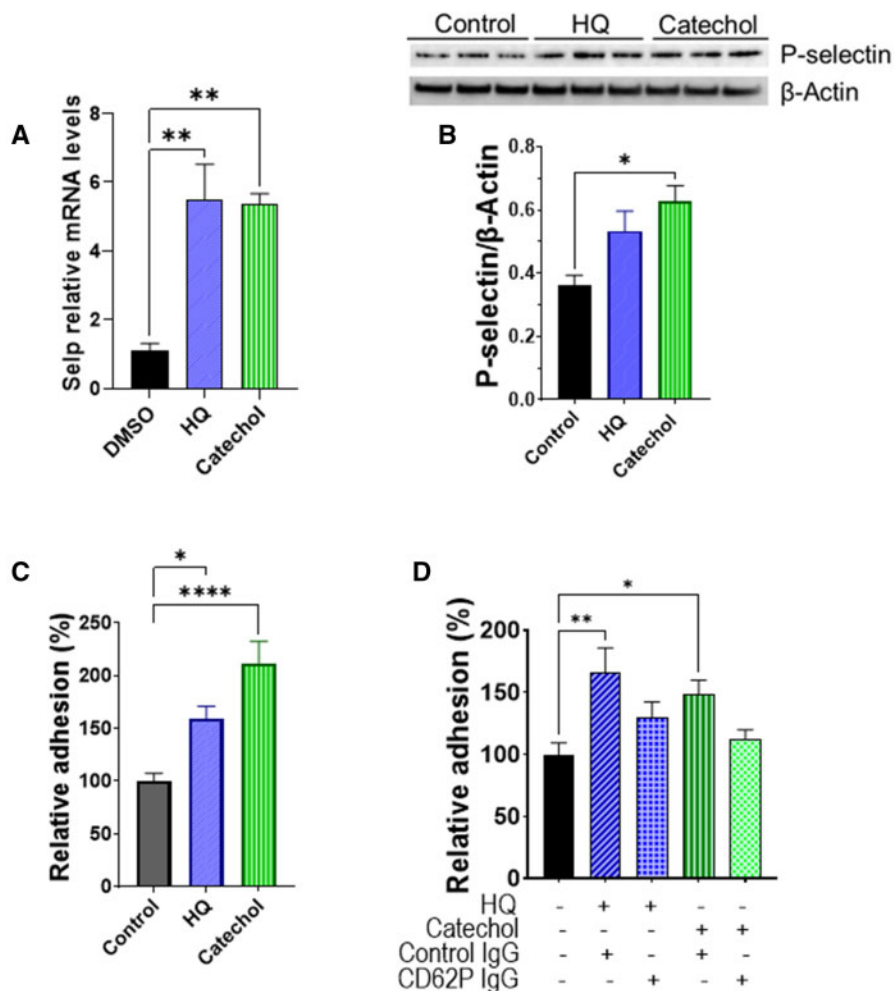


Figure 5. Benzene metabolites induce neutrophil adhesion to the cardiac microvascular endothelial cells (CMVECs). **A**, Transcription of P-selectin (*Selp*) in cardiac microvascular endothelial cells (CMVEC) treated with benzene metabolites hydroquinone (HQ; 5 μ M, 6 h) and catechol (5 μ M, 24 h). **B**, HQ (5 μ M, 24 h)- and catechol (5 μ M, 24 h)-induced upregulation of P-selectin protein in CMVEC. **C**, Adhesion of bone marrow-derived calcein-labeled murine neutrophils to CMVEC pretreated with HQ (5 μ M) and Catechol (5 μ M) for 24 h. **D**, Inhibition of neutrophil adhesion to HQ (5 μ M, 24 h)- and catechol (5 μ M, 24 h)-stimulated CMVEC by anti-P-selectin antibody. Values are mean \pm SEM. * p < .05, ** p < .01, *** p < .001, and **** p < .0001 between corresponding groups analyzed by 1-way ANOVA with Holm-Sidak post hoc test.

2006; Morrow et al., 2008). Overall, increased neutrophil infiltration in the hearts could play a pivotal role in benzene exposure-induced cardiac dysfunction in the pressure overload hearts.

Although precise mechanisms by which benzene exposure exacerbates pressure overload-induced cardiac dysfunction remain unknown, it is plausible that the observed ventricular remodeling of TAC/Benzene mice could, at least in part, be due to the induction of neutrophil gelatinase-associated lipocalin (NGAL or Lcn2) whose expression is regulated by the S100A8/A9 complex (Ichikawa et al., 2011). Lcn2 plays a central role in the ontogeny of cardiac hypertrophy and heart failure (Buonafina et al., 2018; Marques et al., 2017; Yndestad et al., 2004) and can bind Mmp9 to create a complex to stabilize Mmp9 protein and enhance metalloproteinase activity (Nuntagowat et al., 2010; Yan et al., 2001). Such changes could support or promote further ventricular remodeling. Moreover, S100A8/A9 can diminish cardiac myocyte contractility (Boyd et al., 2008). Patients with chronic heart failure have elevated plasma myeloperoxidase levels (Tang et al., 2006), and pharmacological inhibition of myeloperoxidase diminishes leukocyte recruitment, and limits remodeling following myocardial infarction (Ali et al., 2016). Therefore, it is conceivable that the augmented neutrophil

infiltration with subsequent release of MPO and S100A8/A9 heterodimer from activated granulocytes affects ventricular remodeling in TAC/Benzene mice.

Despite the difference in inflammatory markers and cardiac dysfunction, we did not observe a change in cardiomyocyte size or gross accumulation of fibrosis. Changes in myocardial function do not require changes in cardiomyocyte size. Several factors impact inotropic and lusitropic aspects of cardiac function, and these do not require changes in cardiomyocyte size. Hence, it is not surprising that we observed differences in ejection fraction but no differences in cardiomyocyte hypertrophy. Because all groups of TAC mice retained a similar stenotic insult (ie, banding), all TAC mice would have similar stimuli for compensatory cardiomyocyte growth. Yet, it is conceivable that, because of the duration of TAC, the hearts have transitioned from concentric to eccentric hypertrophy, which could involve changes in myocyte length; however, we measured only cross-sectional area, which is standard for the field. Regarding the lack of change in fibrosis, there are several caveats to consider. First, endpoints for fibrosis are crude; it is possible that we lacked the sensitivity to detect changes. Second, the TAC model (in contrast to the infarct model) is characterized by relatively

modest levels of diffuse, interstitial fibrosis. Third, it is conceivable that fibrosis simply did not change among the groups.

Although our *in vitro* studies showed increased transcription of P-selectin on microvascular endothelial cells and neutrophil adhesion to endothelial cells, benzene exposure did not change adhesion molecules' transcription in the naïve (uninstrumented) mice. Nonetheless, it is conceivable that benzene exposure in naïve mice can promote the release of preformed adhesion molecules such as P-selectin from storage granules (eg, Weibel-Palade bodies) and induce endothelial activation. However, in the absence of any significant injury, adhesion of neutrophils to the endothelium is likely to be modest. The pressure overload-induced inflammatory environment and myocardial injury would promote endothelium activation and enhance adhesion of neutrophils to the endothelium in benzene-exposed mice. Increased inflammation in the hearts of mice subjected to pressure overload followed by benzene exposure is further underscored by the increased transcription of chemokines, cytokines, and their receptors (eg, *Il1 β* , *Cxcl1*, and *Cxcr2*). Chemokines such as CXCL1 chemokine are well-known to facilitate neutrophil migration into inflamed tissues (Griffith *et al.*, 2014), promote angiogenesis (Miyake *et al.*, 2013; Scapini *et al.*, 2004) and regulate the recruitment of neutrophils and monocytes during cardiac remodeling and inflammation (Wang *et al.*, 2018). Although the cellular sources (eg, endothelial cells, granulocytes) of CXCL1 and other chemokines and cytokines in the hearts of TAC/benzene-exposed mice remain unknown, they likely augment neutrophil recruitment and migration. Benzene metabolites have been shown to increase the expression of cytokines and chemokines in the peripheral blood mononuclear cells (Gillis *et al.*, 2007) and endothelial cells (Bironaite *et al.*, 2004). Our *in vitro* studies show that in murine CMVECs, benzene metabolites hydroquinone and catechol increase the transcription of chemokine IL-8, which is known to bind to CXCR2 on neutrophils and trigger a signaling cascade that facilitates a firm monocyte adhesion with subsequent intravasation (Gerszten *et al.*, 1999). Further studies are required to delineate the sources of chemokines and cytokines and the molecular mechanisms by which these molecules promote inflammatory signaling in the hearts of TAC/Benzene mice.

Induction of heat shock proteins (HSPs) such as *Hspa1a* and *Hspa1b* in Sham/Benzene hearts appears to be an adaptive response to circumvent inflammatory signaling. Induction of HSPs in response to chemical and mechanical stress enhances protein folding, inhibits inflammation and apoptosis, and provides cytoskeletal protection (Gomez-Pastor *et al.*, 2018). Although little is known about the role of HSPs in pressure overload-induced heart failure, HSF-1, the transcription factor that regulates HSPs is induced by TAC in rats and mice, and constitutive activation of HSF-1 ameliorates TAC-induced cardiac hypertrophy, fibrosis and cardiac dysfunction (Du *et al.*, 2018; Sakamoto *et al.*, 2006; Zhou *et al.*, 2017). Conversely, inhibition of HSF-1 impairs cardiac function in the pressure overload subjected hearts (Sakamoto *et al.*, 2006; Zhou *et al.*, 2017). The HSF-1-mediated cardiac adaptation from pressure overload has been attributed, at least in part, to myocardial angiogenesis via suppression of p53 and subsequent induction of HSF-1 (Zou *et al.*, 2011). HSF-1 can also improve endothelial function (Uchiyama *et al.*, 2007) and prevent inflammatory signaling (Takii *et al.*, 2010). Although the contribution of the HSF-1/HSP axis in the etiology of cardiac dysfunction following TAC/Benzene exposure is unclear, it is likely that these pathways are activated to prevent benzene-induced endothelial activation. Further studies are required to examine the molecular

mechanisms by which HSF-1-dependent transactivation prevents endothelial activation.

Collectively, our studies demonstrate that benzene exposure worsens pressure overload-induced cardiac dysfunction, which is accompanied by increased influx of neutrophils, alterations in cell-cell adhesion, and induction of genes associated with inflammation and stress response. These studies establish the plausibility that benzene exposure is sufficient to exacerbate TAC-induced cardiac dysfunction and provide insight about the underlying mechanisms.

SUPPLEMENTARY DATA

Supplementary data are available at Toxicological Sciences online.

FUNDING

The National Institutes of Health (NIH; grants P42 ES023716, R01 HL149351, R01 HL137229, R01 HL146134, R01 HL156362, R01 HL138992, R01 HL122676, R21 ES033323, U54 HL120163, P30 GM127607, and NIH S10 OD025178) and the Jewish Heritage Foundation grant (OGMN190574L).

DECLARATION OF CONFLICTING INTERESTS

The authors declared no potential conflicts of interest with respect to the research, authorship, and/or publication of this article.

REFERENCES

- Ali, M., Pulli, B., Courties, G., Tricot, B., Sebas, M., Iwamoto, Y., Hilgendorf, I., Schob, S., Dong, A., Zheng, W., *et al.* (2016). Myeloperoxidase inhibition improves ventricular function and remodeling after experimental myocardial infarction. *JACC Basic Transl. Sci.* 1, 633–643.
- An, O., Tan, K. T., Li, Y., Li, J., Wu, C. S., Zhang, B., Chen, L., and Yang, H. (2020). CSI NGS portal: An online platform for automated NGS data analysis and sharing. *Int. J. Mol. Sci.* 21, 3828.
- Appel, B. R., Guirguis, G., Kim, I. S., Garbin, O., Fracchia, M., Flessel, C. P., Kizer, K. W., Book, S. A., and Warriner, T. E. (1990). Benzene, benzo(a)pyrene, and lead in smoke from tobacco products other than cigarettes. *Am. J. Public Health* 80, 560–564.
- Baba, S. P., Zhang, D., Singh, M., Dassanayaka, S., Xie, Z., Jagatheesan, G., Zhao, J., Schmidtke, V. K., Brittan, K. R., Merchant, M. L., *et al.* (2018). Deficiency of aldose reductase exacerbates early pressure overload-induced cardiac dysfunction and autophagy in mice. *J. Mol. Cell Cardiol.* 118, 183–192.
- Bajpai, G., Schneider, C., Wong, N., Bredemeyer, A., Hulsmans, M., Nahrendorf, M., Epelman, S., Kreisel, D., Liu, Y., Itoh, A., *et al.* (2018). The human heart contains distinct macrophage subsets with divergent origins and functions. *Nat. Med.* 24, 1234–1245.
- Bauer, A. K., Faiola, B., Abernethy, D. J., Marchan, R., Pluta, L. J., Wong, V. A., Gonzalez, F. J., Butterworth, B. E., Borghoff, S. J., Everitt, J. I., *et al.* (2003). Male mice deficient in microsomal epoxide hydrolase are not susceptible to benzene-induced toxicity. *Toxicol. Sci.* 72, 201–209.
- Benjamin, E. J., Blaha, M. J., Chiuve, S. E., Cushman, M., Das, S. R., Deo, R., de Ferranti, S. D., Floyd, J., Fornage, M., Gillespie, C., *et*

- al.; American Heart Association Statistics and S. Stroke Statistics. (2017). Heart disease and stroke statistics-2017 update: A Report From the American Heart Association. *Circulation* **135**, e146–e603.
- Bennett, O., Kandala, N. B., Ji, C., Linnane, J., and Clarke, A. (2014). Spatial variation of heart failure and air pollution in Warwickshire, UK: An investigation of small scale variation at the ward-level. *BMJ Open* **4**, e006028.
- Bironaite, D., Siegel, D., Moran, J. L., Weksler, B. B., and Ross, D. (2004). Stimulation of endothelial IL-8 (eIL-8) production and apoptosis by phenolic metabolites of benzene in HL-60 cells and human bone marrow endothelial cells. *Chem. Biol. Interact.* **149**, 177–188.
- Bliksoen, M., Mariero, L. H., Torp, M. K., Baysa, A., Ytrehus, K., Haugen, F., Seljeflot, I., Vaage, J., Valen, G., and Stenslokken, K. O. (2016). Extracellular mtDNA activates NF-kappaB via toll-like receptor 9 and induces cell death in cardiomyocytes. *Basic Res. Cardiol.* **111**, 42.
- Boyd, J. H., Kan, B., Roberts, H., Wang, Y., and Walley, K. R. (2008). S100A8 and S100A9 mediate endotoxin-induced cardiomyocyte dysfunction via the receptor for advanced glycation end products. *Circ. Res.* **102**, 1239–1246.
- Buonafina, M., Martínez-Martínez, E., Amador, C., Gravez, B., Ibarrola, J., Fernández-Celis, A., El Moghrabi, S., Rossignol, P., López-Andrés, N., Jaisser, F., et al. (2018). Neutrophil Gelatinase-Associated Lipocalin from immune cells is mandatory for aldosterone-induced cardiac remodeling and inflammation. *J. Mol. Cell Cardiol.* **115**, 32–38.
- Clayton, C. A., Pellizzari, E. D., Whitmore, R. W., Perritt, R. L., and Quackenboss, J. J. (1999). National Human Exposure Assessment Survey (NHEXAS): Distributions and associations of lead, arsenic and volatile organic compounds in EPA region 5. *J. Exp. Anal. Environ. Epidemiol.* **9**, 381–392.
- Collaborators, G. B. D. R. F. (2016). Global, regional, and national comparative risk assessment of 79 behavioural, environmental and occupational, and metabolic risks or clusters of risks, 1990–2015: A systematic analysis for the Global Burden of Disease Study 2015. *Lancet* **388**, 1659–1724.
- Dassanayaka, S., Zheng, Y., Gibb, A. A., Cummins, T. D., McNally, L. A., Brittan, K. R., Jagatheesan, G., Audam, T. N., Long, B. W., Brainard, R. E., et al. (2018). Cardiac-specific overexpression of aldehyde dehydrogenase 2 exacerbates cardiac remodeling in response to pressure overload. *Redox. Biol.* **17**, 440–449.
- Du, P., Chang, Y., Dai, F., Wei, C., Zhang, Q., and Li, J. (2018). Role of heat shock transcription factor 1(HSF1)-upregulated macrophage in ameliorating pressure overload-induced heart failure in mice. *Gene* **667**, 10–17.
- Frangogiannis, N. G. (2017). The extracellular matrix in myocardial injury, repair, and remodeling. *J. Clin. Invest.* **127**, 1600–1612.
- Fraser, M. P., Cass, G. R., and Simoneit, B. R. T. (1998). Gas-phase and particle-phase organic compounds emitted from motor vehicle traffic in a Los Angeles roadway tunnel. *Environ. Sci. Technol.* **32**, 2051–2060.
- Gerszten, R. E., Garcia-Zepeda, E. A., Lim, Y. C., Yoshida, M., Ding, H. A., Gimbrone, M. A., Jr, Luster, A. D., Luscinskas, F. W., and Rosenzweig, A. (1999). MCP-1 and IL-8 trigger firm adhesion of monocytes to vascular endothelium under flow conditions. *Nature* **398**, 718–723.
- Gillis, B., Gavin, I. M., Arbieva, Z., King, S. T., Jayaraman, S., and Prabhakar, B. S. (2007). Identification of human cell responses to benzene and benzene metabolites. *Genomics* **90**, 324–333.
- Gomez-Pastor, R., Burchfiel, E. T., and Thiele, D. J. (2018). Regulation of heat shock transcription factors and their roles in physiology and disease. *Nat. Rev. Mol. Cell Biol.* **19**, 4–19.
- Griffith, J. W., Sokol, C. L., and Luster, A. D. (2014). Chemokines and chemokine receptors: Positioning cells for host defense and immunity. *Annu. Rev. Immunol.* **32**, 659–702.
- Halade, G. V., Kain, V., and Ingle, K. A. (2018). Heart functional and structural compendium of cardioplemic and cardiorenal networks in acute and chronic heart failure pathology. *Am. J. Physiol. Heart Circ. Physiol.* **314**, H255–H267.
- Healy, A. M., Pickard, M. D., Pradhan, A. D., Wang, Y., Chen, Z., Croce, K., Sakuma, M., Shi, C., Zago, A. C., Garasic, J., et al. (2006). Platelet expression profiling and clinical validation of myeloid-related protein-14 as a novel determinant of cardiovascular events. *Circulation* **113**, 2278–2284.
- Horckmans, M., Ring, L., Duchene, J., Santovito, D., Schloss, M. J., Drechsler, M., Weber, C., Soehnlein, O., and Steffens, S. (2017). Neutrophils orchestrate post-myocardial infarction healing by polarizing macrophages towards a reparative phenotype. *Eur. Heart J.* **38**, 187–197.
- Hutchinson, K. R., Stewart, J. A., Jr, and Lucchesi, P. A. (2010). Extracellular matrix remodeling during the progression of volume overload-induced heart failure. *J. Mol. Cell Cardiol.* **48**, 564–569.
- Ichikawa, M., Williams, R., Wang, L., Vogl, T., and Srikrishna, G. (2011). S100A8/A9 activate key genes and pathways in colon tumor progression. *Mol. Cancer Res.* **9**, 133–148.
- Jacob, P., Abu Raddaha, A. H., Dempsey, D., Havel, C., Peng, M., Yu, L., and Benowitz, N. L. (2013). Comparison of nicotine and carcinogen exposure with water pipe and cigarette smoking. *Cancer Epidemiol. Biomarkers Prev.* **22**, 765–772.
- Kain, D., Amit, U., Yagil, C., Landa, N., Naftali-Shani, N., Molotski, N., Aviv, V., Feinberg, M. S., Goitein, O., Kushnir, T., et al. (2016). Macrophages dictate the progression and manifestation of hypertensive heart disease. *Int. J. Cardiol.* **203**, 381–395.
- Kenyon, E. M., Seaton, M. J., Himmelstein, M. W., Asgharian, B., and Medinsky, M. A. (1998). Influence of gender and acetone pretreatment on benzene metabolism in mice exposed by nose-only inhalation. *J. Toxicol. Environ. Health A* **55**, 421–443.
- Krysko, D. V., Agostinis, P., Krysko, O., Garg, A. D., Bachert, C., Lambrecht, B. N., and Vandenabeele, P. (2011). Emerging role of damage-associated molecular patterns derived from mitochondria in inflammation. *Trends Immunol.* **32**, 157–164.
- Lang, A. L., Chen, L., Poff, G. D., Ding, W. X., Barnett, R. A., Arteil, G. E., and Beier, J. I. (2018). Vinyl chloride dysregulates metabolic homeostasis and enhances diet-induced liver injury in mice. *Hepatol. Commun.* **2**, 270–284.
- Liao, X., Shen, Y., Zhang, R., Sugi, K., Vasudevan, N. T., Alaiti, M. A., Sweet, D. R., Zhou, L., Qing, Y., Gerson, S. L., et al. (2018). Distinct roles of resident and nonresident macrophages in nonischemic cardiomyopathy. *Proc. Natl. Acad. Sci. U.S.A.* **115**, E4661–E4669.
- Lindsey, M. L., Saucerman, J. J., and DeLeon-Pennell, K. Y. (2016). Knowledge gaps to understanding cardiac macrophage polarization following myocardial infarction. *Biochim. Biophys. Acta* **1862**, 2288–2292.
- Lipps, C., Nguyen, J. H., Pyttel, L., Lynch, T. L. t., Liebetau, C., Aleshcheva, G., Voss, S., Dorr, O., Nef, H. M., Mollmann, H., et al. (2016). N-terminal fragment of cardiac myosin binding protein-C triggers pro-inflammatory responses in vitro. *J. Mol. Cell Cardiol.* **99**, 47–56.
- Lloyd-Jones, D. M., Larson, M. G., Leip, E. P., Beiser, A., D'Agostino, R. B., Kannel, W. B., Murabito, J. M., Vasan, R. S., Benjamin, E. J., Levy, D., et al. (2002). Lifetime risk for

- developing congestive heart failure: The Framingham Heart Study. *Circulation* **106**, 3068–3072.
- Ma, Y., Yabluchanskiy, A., Iyer, R. P., Cannon, P. L., Flynn, E. R., Jung, M., Henry, J., Cates, C. A., Deleon-Pennell, K. Y., and Lindsey, M. L. (2016). Temporal neutrophil polarization following myocardial infarction. *Cardiovasc. Res.* **110**, 51–61.
- Marinkovic, G., Grauen Larsen, H., Yndigeegn, T., Szabo, I. A., Mares, R. G., de Camp, L., Weiland, M., Tomas, L., Goncalves, I., Nilsson, J., et al. (2019). Inhibition of pro-inflammatory myeloid cell responses by short-term S100A9 blockade improves cardiac function after myocardial infarction. *Eur. Heart J.* **40**, 2713–2723.
- Marques, F. Z., Prestes, P. R., Byars, S. G., Ritchie, S. C., Wurtz, P., Patel, S. K., Booth, S. A., Rana, I., Minoda, Y., Berzins, S. P., et al. (2017). Experimental and human evidence for lipocalin-2 (neutrophil gelatinase-associated lipocalin [NGAL]) in the development of cardiac hypertrophy and heart failure. *J. Am. Heart Assoc.* **6**, e005971.
- Martini, E., Kunderfranco, P., Peano, C., Carullo, P., Cremonesi, M., Schorn, T., Carriero, R., Termanini, A., Colombo, F. S., Jachetti, E., et al. (2019). Single-cell sequencing of mouse heart immune infiltrate in pressure overload-driven heart failure reveals extent of immune activation. *Circulation* **140**, 2089–2107.
- Miyake, M., Goodison, S., Urquidi, V., Gomes Giacoia, E., and Rosser, C. J. (2013). Expression of CXCL1 in human endothelial cells induces angiogenesis through the CXCR2 receptor and the ERK1/2 and EGF pathways. *Lab. Invest.* **93**, 768–778.
- Morrow, D. A., Wang, Y., Croce, K., Sakuma, M., Sabatine, M. S., Gao, H., Pradhan, A. D., Healy, A. M., Buros, J., McCabe, C. H., et al. (2008). Myeloid-related protein 8/14 and the risk of cardiovascular death or myocardial infarction after an acute coronary syndrome in the Pravastatin or Atorvastatin Evaluation and Infection Therapy: Thrombolysis in Myocardial Infarction (PROVE IT-TIMI 22) trial. *Am. Heart J.* **155**, 49–55.
- Nahrendorf, M., Swirski, F. K., Aikawa, E., Stangenberg, L., Wurdinger, T., Figueiredo, J. L., Libby, P., Weissleder, R., and Pittet, M. J. (2007). The healing myocardium sequentially mobilizes two monocyte subsets with divergent and complementary functions. *J. Exp. Med.* **204**, 3037–3047.
- Nuntagawat, C., Leelawat, K., and Tohtong, R. (2010). NGAL knockdown by siRNA in human cholangiocarcinoma cells suppressed invasion by reducing NGAL/MMP-9 complex formation. *Clin. Exp. Metastasis* **27**, 295–305.
- Patel, B., Bansal, S. S., Ismahil, M. A., Hamid, T., Rokosh, G., Mack, M., and Prabhu, S. D. (2018). CCR2(+) monocyte-derived infiltrating macrophages are required for adverse cardiac remodeling during pressure overload. *JACC Basic Transl. Sci.* **3**, 230–244.
- Patel, B., Ismahil, M. A., Hamid, T., Bansal, S. S., and Prabhu, S. D. (2017). Mononuclear phagocytes are dispensable for cardiac remodeling in established pressure-overload heart failure. *PLoS One* **12**, e0170781.
- Ponikowski, P., Anker, S. D., AlHabib, K. F., Cowie, M. R., Force, T. L., Hu, S., Jaarsma, T., Krum, H., Rastogi, V., Rohde, L. E., et al. (2014). Heart failure: Preventing disease and death worldwide. *ESC Heart Fail.* **1**, 4–25.
- Ran, J., Qiu, H., Sun, S., Yang, A., and Tian, L. (2018). Are ambient volatile organic compounds environmental stressors for heart failure? *Environ. Pollut.* **242**, 1810–1816.
- Ryckman, C., Vandal, K., Rouleau, P., Talbot, M., and Tessier, P. A. (2003). Proinflammatory activities of S100: Proteins S100A8, S100A9, and S100A8/A9 induce neutrophil chemotaxis and adhesion. *J. Immunol.* **170**, 3233–3242.
- Sager, H. B., Hulsmans, M., Lavine, K. J., Moreira, M. B., Heidt, T., Courties, G., Sun, Y., Iwamoto, Y., Tricot, B., Khan, O. F., et al. (2016). Proliferation and recruitment contribute to myocardial macrophage expansion in chronic heart failure. *Circ. Res.* **119**, 853–864.
- Sakamoto, M., Minamino, T., Toko, H., Kayama, Y., Zou, Y., Sano, M., Takaki, E., Aoyagi, T., Tojo, K., Tajima, N., et al. (2006). Upregulation of heat shock transcription factor 1 plays a critical role in adaptive cardiac hypertrophy. *Circ. Res.* **99**, 1411–1418.
- Salvador, A. M., Nevers, T., Velazquez, F., Aronovitz, M., Wang, B., Abadia Molina, A., Jaffe, I. Z., Karas, R. H., Blanton, R. M., and Alcaide, P. (2016). Intercellular adhesion molecule 1 regulates left ventricular leukocyte infiltration, cardiac remodeling, and function in pressure overload-induced heart failure. *J. Am. Heart Assoc.* **5**, e003126.
- Scapini, P., Morini, M., Tecchio, C., Minghelli, S., Carlo, E. D., Tanghetti, E., Albini, A., Lowell, C., Berton, G., Noonan, D. M., et al. (2004). CXCL1/macrophage inflammatory protein-2-induced angiogenesis in vivo is mediated by neutrophil-derived vascular endothelial growth factor-A. *J. Immunol.* **172**, 5034–5040.
- Shioi, T., Matsumori, A., Kihara, Y., Inoko, M., Ono, K., Iwanaga, Y., Yamada, T., Iwasaki, A., Matsushima, K., and Sasayama, S. (1997). Increased expression of interleukin-1 beta and monocyte chemoattractant and activating factor/monocyte chemoattractant protein-1 in the hypertrophied and failing heart with pressure overload. *Circ. Res.* **81**, 664–671.
- Silvestre-Roig, C., Braster, Q., Ortega-Gomez, A., and Soehnlein, O. (2020). Neutrophils as regulators of cardiovascular inflammation. *Nat. Rev. Cardiol.* **17**, 327–340.
- Smith, M. T. (2010). Advances in understanding benzene health effects and susceptibility. *Annu. Rev. Public Health* **31**, 133–148. 132 p following 148.
- Swamydas, M., Luo, Y., Dorf, M. E., and Lionakis, M. S. (2015). Isolation of mouse neutrophils. *Curr. Protoc. Immunol.* **110**, 3.20.1–3.20.15.
- Swirski, F. K., and Nahrendorf, M. (2018). Cardioimmunology: The immune system in cardiac homeostasis and disease. *Nat. Rev. Immunol.* **18**, 733–744.
- Takii, R., Inouye, S., Fujimoto, M., Nakamura, T., Shinkawa, T., Prakasam, R., Tan, K., Hayashida, N., Ichikawa, H., Hai, T., et al. (2010). Heat shock transcription factor 1 inhibits expression of IL-6 through activating transcription factor 3. *J. Immunol.* **184**, 1041–1048.
- Tang, W. H., Brennan, M. L., Philip, K., Tong, W., Mann, S., Van Lente, F., and Hazen, S. L. (2006). Plasma myeloperoxidase levels in patients with chronic heart failure. *Am. J. Cardiol.* **98**, 796–799.
- Tsai, D. H., Wang, J. L., Chuang, K. J., and Chan, C. C. (2010). Traffic-related air pollution and cardiovascular mortality in central Taiwan. *Sci. Total. Environ.* **408**, 1818–1823.
- Uchiyama, T., Atsuta, H., Utsugi, T., Oguri, M., Hasegawa, A., Nakamura, T., Nakai, A., Nakata, M., Maruyama, I., Tomura, H., et al. (2007). HSF1 and constitutively active HSF1 improve vascular endothelial function (heat shock proteins improve vascular endothelial function). *Atherosclerosis* **190**, 321–329.
- Vandal, K., Rouleau, P., Boivin, A., Ryckman, C., Talbot, M., and Tessier, P. A. (2003). Blockade of S100A8 and S100A9 suppresses neutrophil migration in response to lipopolysaccharide. *J. Immunol.* **171**, 2602–2609.

- Villeneuve, P. J., Jerrett, M., Su, J., Burnett, R. T., Chen, H., Brook, J., Wheeler, A. J., Cakmak, S., and Goldberg, M. S. (2013). A cohort study of intra-urban variations in volatile organic compounds and mortality, Toronto, Canada. *Environ. Pollut.* **183**, 30–39.
- Wang, L., Zhang, Y. L., Lin, Q. Y., Liu, Y., Guan, X. M., Ma, X. L., Cao, H. J., Liu, Y., Bai, J., Xia, Y. L., et al. (2018). CXCL1-CXCR2 axis mediates angiotensin II-induced cardiac hypertrophy and remodelling through regulation of monocyte infiltration. *Eur. Heart J.* **39**, 1818–1831.
- Wang, Y., Sano, S., Oshima, K., Sano, M., Watanabe, Y., Katanasaka, Y., Yura, Y., Jung, C., Anzai, A., Swirski, F. K., et al. (2019). Wnt5a-mediated neutrophil recruitment has an obligatory role in pressure overload-induced cardiac dysfunction. *Circulation* **140**, 487–499.
- Ward, C. O., Kuna, R. A., Snyder, N. K., Alsaker, R. D., Coate, W. B., and Craig, P. H. (1985). Subchronic inhalation toxicity of benzene in rats and mice. *Am. J. Ind. Med.* **7**, 457–473.
- Watson, L. J., Facundo, H. T., Ngho, G. A., Ameen, M., Brainard, R. E., Lemma, K. M., Long, B. W., Prabhu, S. D., Xuan, Y. T., and Jones, S. P. (2010). O-linked beta-N-acetylglucosamine transferase is indispensable in the failing heart. *Proc. Natl. Acad. Sci. U.S.A.* **107**, 17797–17802.
- Watson, L. J., Long, B. W., DeMartino, A. M., Brittan, K. R., Readnower, R. D., Brainard, R. E., Cummins, T. D., Annamalai, L., Hill, B. G., and Jones, S. P. (2014). Cardiomyocyte Ogt is essential for postnatal viability. *Am. J. Physiol. Heart. Circ. Physiol.* **306**, H142–153.
- Weinberger, T., and Schulz, C. (2015). Myocardial infarction: A critical role of macrophages in cardiac remodeling. *Front. Physiol.* **6**, 107.
- Weisheit, C., Zhang, Y., Faron, A., Kopke, O., Weisheit, G., Steinstrasser, A., Frede, S., Meyer, R., Boehm, O., Hoeft, A., et al. (2014). Ly6C(low) and not Ly6C(high) macrophages accumulate first in the heart in a model of murine pressure-overload. *PLoS One* **9**, e112710.
- Wilhelmsen, K., Farrar, K., and Hellman, J. (2013). Quantitative in vitro assay to measure neutrophil adhesion to activated primary human microvascular endothelial cells under static conditions. *J. Vis. Exp.* **78**, e50677.
- Wong, O., and Fu, H. (2005). Exposure to benzene and non-Hodgkin lymphoma, an epidemiologic overview and an ongoing case-control study in Shanghai. *Chem. Biol. Interact.* **153-154**, 33–41.
- Yan, L., Borregaard, N., Kjeldsen, L., and Moses, M. A. (2001). The high molecular weight urinary matrix metalloproteinase (MMP) activity is a complex of gelatinase B/MMP-9 and neutrophil gelatinase-associated lipocalin (NGAL). Modulation of MMP-9 activity by NGAL. *J. Biol. Chem.* **276**, 37258–37265.
- Yndestad, A., Ueland, T., Oie, E., Florholmen, G., Halvorsen, B., Attramadal, H., Simonsen, S., Froland, S. S., Gullestad, L., Christensen, G., et al. (2004). Elevated levels of activin A in heart failure: Potential role in myocardial remodeling. *Circulation* **109**, 1379–1385.
- Zhou, N., Ye, Y., Wang, X., Ma, B., Wu, J., Li, L., Wang, L., Wang, D. W., and Zou, Y. (2017). Heat shock transcription factor 1 protects against pressure overload-induced cardiac fibrosis via Smad3. *J. Mol. Med. (Berl.)* **95**, 445–460.
- Zou, Y., Li, J., Ma, H., Jiang, H., Yuan, J., Gong, H., Liang, Y., Guan, A., Wu, J., Li, L., et al. (2011). Heat shock transcription factor 1 protects heart after pressure overload through promoting myocardial angiogenesis in male mice. *J. Mol. Cell Cardiol.* **51**, 821–829.